

Article

A Convenient and Efficient Strategy for Improving Separation Ability of Capillary Electrophoresis Through Tilting Capillary as Needed

Wenhui Jia, Pingyi Zheng, Yuchen Cui, James J. Bao, Yanmei Xu and Youxin Li * 

Tianjin Key Laboratory for Modern Drug Delivery and High-Efficiency, Collaborative Innovation Center of Chemical Science and Engineering, School of Pharmaceutical Science and Technology, Faculty of Medicine, Tianjin University, 92 Weijin Road, Nankai District, Tianjin 300072, China; jiawenhui1996@163.com (W.J.); m18804096535_1@163.com (P.Z.); cyc166004854282024@163.com (Y.C.); bao@biomicsinc.com (J.J.B.); 13785197771@163.com (Y.X.)

* Correspondence: lyx@tju.edu.cn

Abstract: The effect of gravity based on the vector sum of gravity and buoyancy forces working spontaneously for all species was introduced into capillary electrophoresis (CE) as another important force which cooperated with electrophoretic flow and electro-osmotic flow. Their portion was adjusted by simply tilting the whole of the capillary at an angle during CE running. The related formula was proposed and verified through a series of experiments. After investigating the related parameters, results showed that the gravity effect was significantly affected by additives in the buffer, the length, and the inner diameter of the capillary, and the size of the sample molecule. This made the different ions with opposite or significantly different mobilities to be observed at a CE run. It significantly improved separation efficiencies of some small molecules, chiral compounds, macromolecules and cells when the tilt angles of the capillary were adjusted to a special range predicted through the fitting curve. In addition, micrometer level microspheres and cells were firstly separated by the new CE strategy and the resolutions were more than 1.0. After ingeniously designing the gradient of the tilting angle with time, we were able to further enhance the separation efficiency of the targets. For example, the resolution of lysozyme and ribonuclease A could be increased from 3.691 to 7.342. These indicated the huge potential of the new CE strategy and its gradient mode in separation.

Keywords: capillary electrophoresis; gravity; buoyancy force; gravity effect; gradient capillary electrophoresis; separation technology



Citation: Jia, W.; Zheng, P.; Cui, Y.; Bao, J.J.; Xu, Y.; Li, Y. A Convenient and Efficient Strategy for Improving Separation Ability of Capillary Electrophoresis Through Tilting Capillary as Needed. *Separations* **2024**, *11*, 340. <https://doi.org/10.3390/separations11120340>

Academic Editor: Gavino Sanna

Received: 24 October 2024

Revised: 19 November 2024

Accepted: 25 November 2024

Published: 27 November 2024



Copyright: © 2024 by the authors. Licensee MDPI, Basel, Switzerland. This article is an open access article distributed under the terms and conditions of the Creative Commons Attribution (CC BY) license (<https://creativecommons.org/licenses/by/4.0/>).

1. Introduction

Since the emergence of capillary electrophoresis (CE) in 1981, it has been proven to be a versatile and useful separation technique with significantly high efficiency [1,2]. In CE, electro-osmotic flow (EOF) drives the bulk liquid through the capillary. In addition, the charged species have their own electrophoretic flow (EP). The overall flow of a specific ion is the vector sum of both EOF and EP. Generally, the magnitude of EOF is relatively high, at about 5–7 times as much as electrophoretic flow. On the one hand, it conveniently drives most of a species to move in the same direction; however, it also brings some separation difficulties. For example, it is hard to separate those similar ions in a finite length channel if their mobilities are relatively close. Of course, part of the separation cases may be solved through optimizing electrophoretic conditions which affect both EP and EOF [3]. Separation may also be improved through changing the EOF, which could be restrained through coating or adding surfactant into the buffer [4]. However, there are still some cases where the targets cannot be separated well, based on current CE technology. Thus, it is desirable to introduce a different strategy to improve the separation efficiency and/or selectivity. On the other hand, the effect of EOF is weak in some cases. If the apparent

mobilities of partial analytes are opposite and greatly different from other analytes, they will migrate toward different directions so that they cannot be determined in a CE run. In addition, it is also hard for EOF to drive particles (like cell, microsphere) and this issue is further deteriorated by absorption and precipitation phenomena. Thus, it is urgent to introduce another driven force to solve the above issues.

At present, various methodologies have been explored to introduce external forces into CE, such as external field, chemical, and pressure introduction. The external electrical field perpendicular to the capillary was used to alter the internal double layer on the surface of the inner capillary wall [5–8]. However, the effect of this type of alteration is very limited, especially when the silanols on the silica surface are modified by organic groups. This makes it hard to take advantage of this force to directly influence the separation performance [5,9–13]. As for chemical introduction, employing different background electrolytes, especially adding some cation surfactants, can reduce or eliminate EOF, or even change its direction [14]. The modification to the inner wall of the capillary is also adopted to change EOF [15]. Although it cannot directly improve the difference between electrophoretic mobilities, it allows the ions exhibit their differences on apparent mobilities in CE. However, in a CE run, the force from chemical introduction cannot be adjusted arbitrarily as needed. Another means of adjusting the movement of ionic species inside the capillary is to use pressure [16]. It has the advantages of easy operation, strong adjustability in time, and low cost. At the same time, it does not require an external electric field or chemical reagents, which means it can avoid the complex impact. When pressure is introduced from the opposite direction, only the ions with residual apparent mobilities remain for movement and the separation can be enhanced or completed in a short-capillary [17]. Microchips, which have very limited flow path lengths are good examples for this type of pressure approach [18,19]. For practical reasons, a special injection valve was made [20] to make flow-counterbalanced CE commercially attractive [21]. Vigh and others developed several pressure-mediated methods for rapidly measuring the mobilities [9,22], which were further used for measuring the effective mobilities, chiral separation selectivity from partially separated enantiomer peaks in a racemic mixture [23,24] and eliminating chromatographic bias [25]. Moreover, they used pressure to determine isoelectric points of ampholytes with closely spaced pKa values [26]. With the assistance of a constant pressure, CE was applied in some applications, such as the analysis of multivalent anions [27] or cations [28], nucleotides [29], and aggregates [30]. Our group also utilized pressure to push all of the substances into a constant temperature region and performed affinity CE to measure protein binding constants [31], which was also done using frontal analysis [32]. Pressure also was employed in an automated hydrodynamically mediated technique for the preparation of calibration solutions [33]. B. A. Williams, Jr. contributed to the theoretical basis of the approach [34] and conducted a comprehensive study of pressure-mediated CE [35]. Jorgenson reported a flow-counterbalanced capillary electrophoresis (FCCE) approach in 1994 [36]. The aforementioned examples demonstrated that pressure could play a role in the quantitation of analyte, the determination of a variety of analyte parameters, and even be used for the preparation of reagents. However, for pressure to be useful in separation, it is necessary to dynamically control the level and magnitude of the applied pressure. Even more, the need for dynamically controlling the pressure to form a much-needed gradient presents a significant challenge in implementing this technique. So far, there are methods available to apply pressure to CE [24,32–35], but most of them do not really utilize pressure as another force like EOF and EP to significantly affect separation due to the fact that they are hard to real-time smoothly, and to rapidly adjust the tiny pressure as needed. Thus, they have not attracted widespread attention, applications and further development.

Gravity is directly ignored for small molecules separation in CE. In many CE applications, it is viewed as an adverse factor because it easily induces the precipitation of macromolecules (like protein) and aggravates their absorption issue to the capillary wall. There were some so-called gravity-mediated CE methods, which were to put a container with liquid at one of end of the capillary [37,38], and converted gravity into pressure to

push the whole of the liquid flow. For example, Wang et al. [37] converted into pressure through setting a 0.2 mL microtubes with 0.8 cm liquid height at the injection end of a capillary to push dopamine and catechol, resulting in a decreased resolution from 3.6 to 1.6 under 800 V voltage and a changed ΔH from 0 cm to 0.8 cm. It is a good example to verify that hydrostatic pressure may be not conducive to separation in this situation.

Our strategy is to utilize the spontaneous vertical falling behavior of each substance through a tilting capillary to produce another force which is accompanied by buoyancy force in a CE running buffer. If substances have different density, their velocities may be different. This is never studied. We found it was useful in some chiral separations [39]. However, the basic theory is not systematically analyzed and the applications need to be expanded. Here, we proposed and validated the related theory about the introduction of the gravity effect or its portion as the third important force into CE through a tilting capillary. In the novel CE mode, the migration of species will be co-affected by EOF, EP, buoyancy force and portion of their own gravity. In theory, (1) the apparent mobility difference between two ions with similar EP maybe increased; (2) it can effectively solve the precipitation issue, especially for macromolecules. Even so, it can make it possible to separate particles in CE. (3) the net force can be timely and smoothly changed by tilting the capillary at a different angle as CE separation is needed. To validate these, we investigated the suitable scale of tilt angle. In the effective tilting angle scale, its gradient mode, i.e., the change of tilting angle over time was also tried. The novel CE technology was applied in separations of small molecules, macromolecules, chiral compounds, particles and cells to extend the CE application range and ability.

2. Theory

2.1. Migration of Species in CE

The migration of an ionic species in traditional CE involves two components: EOF and EP. EOF is the bulk movement while EP is the migration of the ion under electric field. The apparent electrophoretic velocity (v_{ap}) of a species inside the capillary is the vector sum of both electroosmotic velocity (v_{EOF}) and electrophoretic velocity (v_{ep}), i.e.,:

$$v_{ap} = v_{EOF} + v_{ep} = \frac{l}{t} \quad (1)$$

where l is the effective length (the length from injection to detection window), and t is the migration time.

The total mass, m , inside a capillary of length (L) and inner radius (r_c) filled with a liquid of density (ρ) is:

$$m = \rho V = \rho \pi r_c^2 L \quad (2)$$

Normally, gravity is perpendicular to the ground while most CE was run horizontally. Even if the capillary has a certain curvature, the effect of gravity is ignored because the two ends of the capillary are required in the same horizontal line. However, if the capillary is purposely vertical, the gravity force, F_g , of the liquid inside the capillary is:

$$F_g = mg = \rho g \pi r_c^2 L \quad (3)$$

where g is the earth's gravity, $g = 9.80665 \text{ m.s}^{-2}$. If buoyancy force is ignored and the whole of the capillary is tilted, θ , it will create an imbalanced gravity force with the downward portion of gravity force as capillary direction, $F_{g,v}$:

$$F_{g,v} = F_g \sin \frac{\pi \theta}{180} = \rho g \pi r_c^2 L \sin \frac{\pi \theta}{180} \quad (4)$$

The portion of gravity will result in movement of targets inside the capillary. For a spherical analyte, if its own gravity velocity was equal to the gravity velocity of the filled liquid in capillary, its apparent velocity can be expressed as:

$$v_{ap-g} = v_{g,v} + v_{EOF} + v_{ep} = \frac{\rho g \pi r_c^2 L \sin \frac{\pi \theta}{180}}{6 \pi \eta r} + v_{EOF} + v_{ep} = \frac{\rho g r_c^2 L \sin \frac{\pi \theta}{180}}{6 \eta r} + v_{EOF} + v_{ep} \quad (5)$$

where $v_{g,v}$ is the gravity-driven velocity, and v_{ap-g} is the apparent velocity under gravity. From the equation, it is obvious the gravity term relates with the density and viscosity of the running buffer, the tilt angle, radius and length of the capillary, and the radius of the spherical analyte. When the running buffer, capillary and analyte are fixed and the hypothesis is that there is no viscosity change in the running buffer in CE; it only relates to the capillary tilt angle.

If the buoyancy force of a spherical analyte itself (like cell, microsphere) was more or less than the gravity velocity, its movement would be different. It relates with its own density, particle radius, capillary tilt angle, the density and viscosity of the running buffer, etc. In this situation, it is possible to separate two analysts with large differences in density through a tilting capillary.

In either case, the bulk or individual movement is called the gravity effect (GE) and the apparent velocity of the analyst in CE is simply rewritten as:

$$v_{ap-g} = G \sin \frac{\pi \theta}{180} + v_{EOF} + v_{ep} \quad (6)$$

where G stands for the fixed value when electrophoretic conditions except the tilt angle of the capillary are fixed.

The apparent mobility of analyte (μ_{ap-g}) is expressed as:

$$\mu_{ap-g} = \frac{v_{ap-g}}{E} = \frac{G \sin \frac{\pi \theta}{180} + v_{EOF} + v_{ep}}{E} = G' \sin \frac{\pi \theta}{180} + \mu_{EOF} + \mu_{ep} \quad (7)$$

where G' is a constant value when electrophoretic conditions excepting the capillary tilt angle are fixed.

2.2. Apparent Mobility Change with Capillary Tilt Angle and Its Application Strategy

It is clear that the gravity effect has no benefit on selectivity and resolution if CE is carried out in the conventional horizontal format. However, if the capillary is tilted and other parameters are constants, the gravity effect will change as a function of the tilt angle, which may have a significant impact on μ_{ap-g} . At different angles, the apparent mobilities of different compounds will change accordingly.

When the portion of gravity and buoyancy force is in the same direction as the vector sum of EOF and EP, the apparent mobility increases. When they are opposite, μ_{ap-g} decreases. To explain this clearly, two model compounds with positive charge were exemplified and the initial mobilities of compound A and compound B were assumed to be 6 units and 4 units, respectively. Their mobility changes as a function of angles were simulated through a commercial simulation software, which is 1stOpt15PRO from 7D-Soft High Tech. Inc. (Beijing, China). The simulated results are shown in Figure 1.

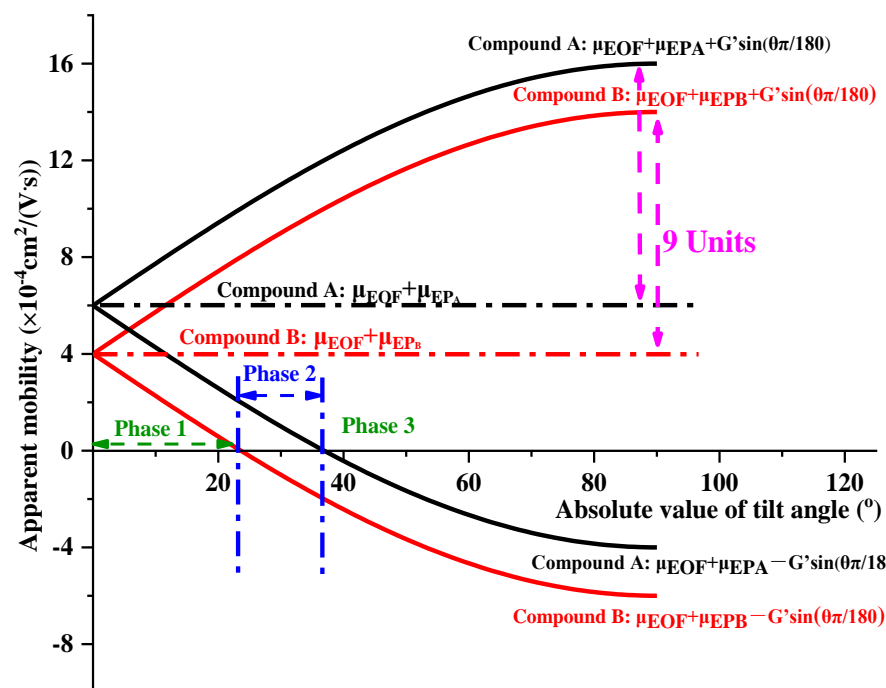


Figure 1. The simulated apparent mobility changes of model compound A and compound B as capillary tilt angles.

According to the theory (Equation (7)) and the actual variation range of the apparent mobility, the mobility for each of them changes as a function of the tilt angle with a range between the highest and the lowest of 9 units. However, the mobilities of compound A and compound B always change simultaneously with a constant difference of 2 units, and have no cross or overlap within $+90^\circ$ angle in apparent mobility values. Thus, it is difficult to improve the separation of compound A from compound B in a fixed capillary by simply changing the tilt angle. Looking more into the details, in the bottom part of Figure 1 ($0^\circ \sim -90^\circ$), they are more complicated as it contains three phases where the vector sum of EOF and EP is in different directions under gravity effect: Phase 1: $0^\circ \sim -23.2^\circ$, both compound A and compound B move in the same directions with a constant difference of mobilities. Phase 2: $-23.2^\circ \sim -36.8^\circ$, compound A and compound B move in opposite directions. The apparent mobility of compound B is 0 at -23.2° , which intercepts with the horizontal axis. After that point, its migration direction becomes negative, i.e., moving in the opposite direction. While the migration direction of compound A does not change before -36.8° . At -36.8° , compound A stops. It indicates that the two compounds have their zero-mobility points at -23.2° or -36.8° , respectively. Between -23.2° and -36.8° , they will move in opposite directions. Therefore, this is the range that can be used to greatly improve their separation by making one of them stop or migrate in opposite directions. Phase 3: $-36.8^\circ \sim -90^\circ$, similar to Phase 1, both compound A and compound B move toward a negative direction at a constant mobility difference. Therefore, Phase 2 is the useful scale of tilting angle that can be utilized to enhance separation. For this purpose, there are two ways to enhance the separation: the zero mobility (ZM) method and the opposite mobility (OM) method.

In the ZM method, there are two tilt angles where one species moves at a mobility of zero while the other stops at a non-zero mobility. In the case of Figure 1, compound B has a net mobility of zero at -23.2° . At this tilt angle, compound A moves at a mobility of 2 units, but compound B stops. The longer duration time, the farther compound A moves, and the more significant the gravity effect. Similarly, compound A has a zero mobility at -36.8° where compound B moves at a rate of -2 units. In this ZM mode, the similar movement could be observed but compound B keeps moving oppositely and compound A stops.

In the OM method, between -23.2° and -36.8° , compound A and compound B move in different directions. When the negative tilt angle increases in the bottom of Figure 1, compound A migrates more and more slowly, while compound B migrates more and more quickly to the opposite direction. The gravity effect is gradually obvious for compound A and compound B. Their position gap and resolution simply increase as a function of time. This reminds us that the tilt angle should be adjusted according to the analytes.

As electrophoresis conditions change, the initial vector sum of EOF and EP will be different. Depending on the relative mobility of two ions, there are multiple situations if they moved in opposite directions. To graphically describe the various situations, a series of mobility changes as capillary tilt angle and zero mobility were constructed when the initial mobility changed between $-10 \times 10^{-4} \text{ cm}^2/(\text{V.s})$ and $10 \times 10^{-4} \text{ cm}^2/(\text{V.s})$. The above situations based on the fact that the magnitude of the gravity effect, $\sim 9 \times 10^{-4} \text{ cm}^2/(\text{V.s})$, would have a significant impact on typical apparent mobility ($< 6 \times 10^{-4} \text{ cm}^2/(\text{V.s})$). Each case is summarized in Table 1. Between the initial apparent mobility of $-10 \times 10^{-4} \text{ cm}^2/(\text{V.s})$ to $10 \times 10^{-4} \text{ cm}^2/(\text{V.s})$, there were no situations where the curve did not pass the zero line. To verify the above theory, a series of experiments were performed. The details were as follows:

Table 1. Different situations of opposite mobility (OM) mode.

Sum of Electrophoretic and Electroosmotic Mobility ($\text{cm}^2/(\text{V.s})$)	Zero Mobility	Opposite Migration	Meaningful Adjustment of Capillary Tilt Angle
$\mu_{0,A} > 10^{-3}; \mu_{0,B} > 10^{-3}$	No	No	No
$\mu_{0,A} > 10^{-3}; \mu_{0,B} = 10^{-3}$	Yes, B	No	Yes
$\mu_{0,A} = 10^{-3}; 0 < \mu_{0,B} < 10^{-3}$	Yes, A, B	Yes	Yes
$0 < \mu_{0,A} < 10^{-3}; 0 < \mu_{0,B} < 10^{-3}$	Yes, A, B	Yes	Yes
$0 < \mu_{0,A} < 10^{-3}; \mu_{0,B} = 0$	Yes, A, B	Yes	Yes
$\mu_{0,A} = 0; -10^{-3} < \mu_{0,B} < 0$	Yes, A, B	Yes	Yes
$-10^{-3} < \mu_{0,A} < 0; -10^{-3} < \mu_{0,B} < 0$	Yes, A, B	Yes	Yes
$-10^{-3} < \mu_{0,A} < 0; \mu_{0,B} = -10^{-3}$	Yes, A, B	Yes	Yes
$\mu_{0,A} = -10^{-3}; -10^{-3} < \mu_{0,B} < 0$	Yes, A	No	Yes
$\mu_{0,A} < -10^{-3}; \mu_{0,B} < -10^{-3}$	No	No	No

3. Experimental

3.1. Chemicals and Reagents

Sodium hydroxide (NaOH, 96%) was from Hengshan Chemical Technology (Tianjin, China). Hydrochloric acid (HCl, 36~38%) and phosphoric acid (H_3PO_4 , 85%) were from Lianlong Bohua Medicinal (Tianjin, China). Sodium dihydrogen phosphate (NaH_2PO_4 , 97%) and disodium hydrogen phosphate (Na_2HPO_4 , 99%) were from Heowns Biochem LLC (Tianjin, China). Diphenylguanidine (99.5%), trisodium phosphate (Na_3PO_4 , 98%), hydroxypropyl methyl cellulose (HPMC, 95%, MW 20,000), sodium dodecyl sulfate (SDS, 95%, MW 20,000) and hexadecyl trimethyl ammonium bromide (CTAB, 95%, MW 20,000) were from Damao Chemical Reagents (Tianjin, China). Benzoic acid (99.5%) and polyethylene glycol (PEG, 95%, MW 10,000) were from Yuanli Chemical (Tianjin, China). Acetonitrile (ACN, 99.9%) was from OCEANPAK (Gothenburg, Sweden) and p-toluenesulfonic acid (99.5%) was from Kewei (Tianjin, China). Acetic acid (CH_3COOH , 99.5%) and sodium acetate (CH_3COONa) were from Ji'Erzheng Chemical Trade (Tianjin, China). Bovine serum albumin (BSA, 96%) was from Gen-view Scientific (Poway, CA, USA). Ribonuclease A (RNase A, 70 units/mg) was from Sigma-Aldrich (St. Louis, MO, USA). Lysozyme (LZ, from chicken egg white, 7000 units/mg) was from Huamaike Biotechnology (Beijing, China). Polystyrene-divinylbenzene microspheres (PS-DVB), polystyrene-divinylbenzene microspheres-COCl (PS-DVB-COCl), polystyrene-divinylbenzene microspheres- SO_3H (PS-DVB- SO_3H), polystyrene-divinylbenzene microspheres- $\text{N}^+(\text{CH}_3)_3$ (PS-DVB- $\text{N}^+(\text{CH}_3)_3$) with the size of 5 μm , and sulfated β -cyclodextrin polymer (SPE- β -CDP, MW > 7000)

were homemade. All of the other chemicals and reagents were from Jiangtian Chemical Technology (Tianjin, China). Deionized water (DI water) was from Yongqingyuan Distilled Water Business Department (Tianjin, China).

3.2. Instrumentation

CE experiments were performed in a CE apparatus equipped with a Spectra 100 full wavelength UV detector (SP, Santa Clara, CA, USA) and a direct current (DC) power supply (Model HB-Z153-3AC, Zhejiang Hengbo Electrical Appliance Manufacturing Co., Ltd., Wenzhou, China). Data were collected by an N-2000 workstation (Institute of Intelligent Information, Zhejiang University, Hangzhou, China). The capillary was from Yongnian Optical (Handan, China). The detector-installed capillary was placed in a home-made holder and could be rotated as shown in Figure 2. The elevation of capillary B end was recorded as positive angle “+”, and the decline of capillary B end was recorded as negative angle “−”.

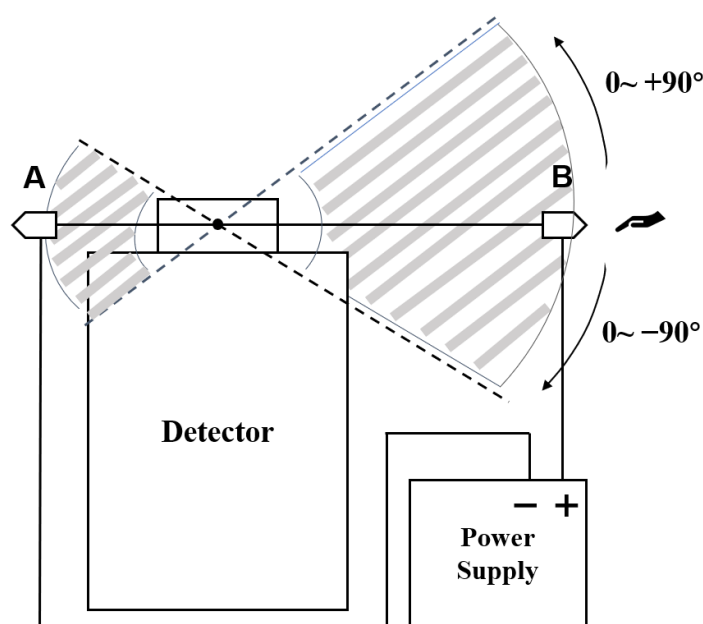


Figure 2. Diagram of the rotatable CE instrumentation (the B end is the injection end).

3.3. Electrophoresis Conditions

A new capillary was treated with 0.1 mol/L NaOH, 0.1 mol/L HCl and DI water for 30 min, respectively. Then, the capillary was rinsed with buffer to equilibrium. Between runs, the capillary was rinsed by 0.1 mol/L NaOH and buffer for 1 min. Unless otherwise stated, electrophoretic conditions were as follows. The capillary was an uncoated capillary with outer diameter/inside diameter (OD/ID) 350/75 μm . Capillary total/effective lengths were 47/33 cm or 47/14 cm. Voltage was 10,000 V. Detection wavelength was 214 nm. The sample was injected through the gravity injection method with a duration of 2 s.

3.4. Data Analysis

The relationship between the apparent mobility and the capillary tilt angle was simulated by using a commercial simulation software, which is 1stOpt15PRO from 7D-Soft High Tech. Inc. (Beijing, China).

4. Results and Discussion

4.1. Parameters of the Gravity-Mediated Capillary Electrophoresis

In CE, the apparent mobility is related to several parameters, such as pH value, ionic strength and additives in buffer, length and inner diameter of capillary, analyte species, and even size of sample molecule. To investigate the relationship between these parameters

and gravity effect, a series of experiments without voltage were designed and performed, which excluded the effect of electrophoretic force. Phosphate and acetate buffer solutions of 15.0 mM pH 4.0 were used as different types of running buffers. Phosphate buffers of 15.0 mM at pH 2.0–8.0 were prepared for pH effect. Phosphate buffers (pH 4.0) of 15.0 mM, 100.0 mM and 200.0 mM were made for ionic strength effect. Different additives including 0.1% (v/v) ACN, 0.05% (m/v) HPMC, 0.1% (m/v) SDS or 0.1% (m/v) CTAB were added into 15.0 mM of phosphate buffer (pH 4.0), respectively, to investigate the viscosity effect. Capillary lengths of 47, 37 and 27 cm with effective lengths of 33, 23, and 13 cm, respectively, were employed to investigate the capillary length effect. The 50, 75, 100, 150, and 250 μm inner diameters of capillaries were tested to obtain the capillary inner diameter effect. In the above experiments, 0.3% (v/v) DMSO aqueous solution was chosen as the analyte. In testing the effect of molecular size, 0.3% (v/v) DMSO aqueous solution, 0.1 mg/mL BSA, and 0.1 mg/mL PS-DVB microspheres of 5 μm were used as small, large molecules and particle analytes, respectively. All the above experiments were performed with the capillary tilt at 30°, 60° and 90°, respectively.

Based on their effectiveness on gravity effect (see Figures S1–S3 and 3), these parameters could be divided into two groups. The first group was low-impact parameters including buffer type, pH value and ion strength. As could be seen in Figures S1–S3, the three parameters had little or no influence on gravity effect as the relative standard deviations (RSD) in migration velocity was less than 5%. The reason may be the similar viscosity of the buffers. The strong-impact parameters were shown in Figure 3a–d, where their RSDs in migration velocity were more than 5%. Figure 3a showed the effect of additives. Without polymers, the migration time was relatively short. The addition of ACN, SDS, CTAB, or HPMC increased the migration time of the analyte due to the increase of viscosity in turn and charge change on the surface of the capillary. It was shown that adjusting the viscosity of the buffer would have a significant impact on gravity effect. Figure 3b showed the change of capillary lengths from 33 cm to 13 cm resulted in a decrease in velocity. It was known that lengthening or shortening the length of the capillary was actually changing the height difference between the two ends of the capillary, which would change the effect of gravity. Because the gravity velocity of DMSO was similar to the bulk movement speed, it would be affected by capillary length and reduce as the capillary shortened. As the inner diameter decreased, the migration time of DMSO increased (see Figure 3c). The larger the inner diameter, the smaller the relative contact area between the bulk flow and the inner wall, resulting in the smaller the resistance received, so the gravity effect was more significant. Figure 3d showed that different sizes of molecules afforded different gravity effects. The migration times of the three substances were quite different at the same angle. At 30°, small molecule DMSO had the shortest migration time, followed by PS-DVB and BSA. However, at 60°, the difference between the three species decreased, possibly due to the large inclination angle, and the gravity effect tended to be uniform, so that the influence of molecular size on migration time was weakened. At 90°, the conclusions coincided with those at 60°. These results indicated that the gravity effect was significantly affected by additives in buffer, length and inner diameter of the capillary, and size of the sample molecule. Moreover, when the properties of two analytes were large enough, it was possible to separate them under the gravity effect (see Figure S4).

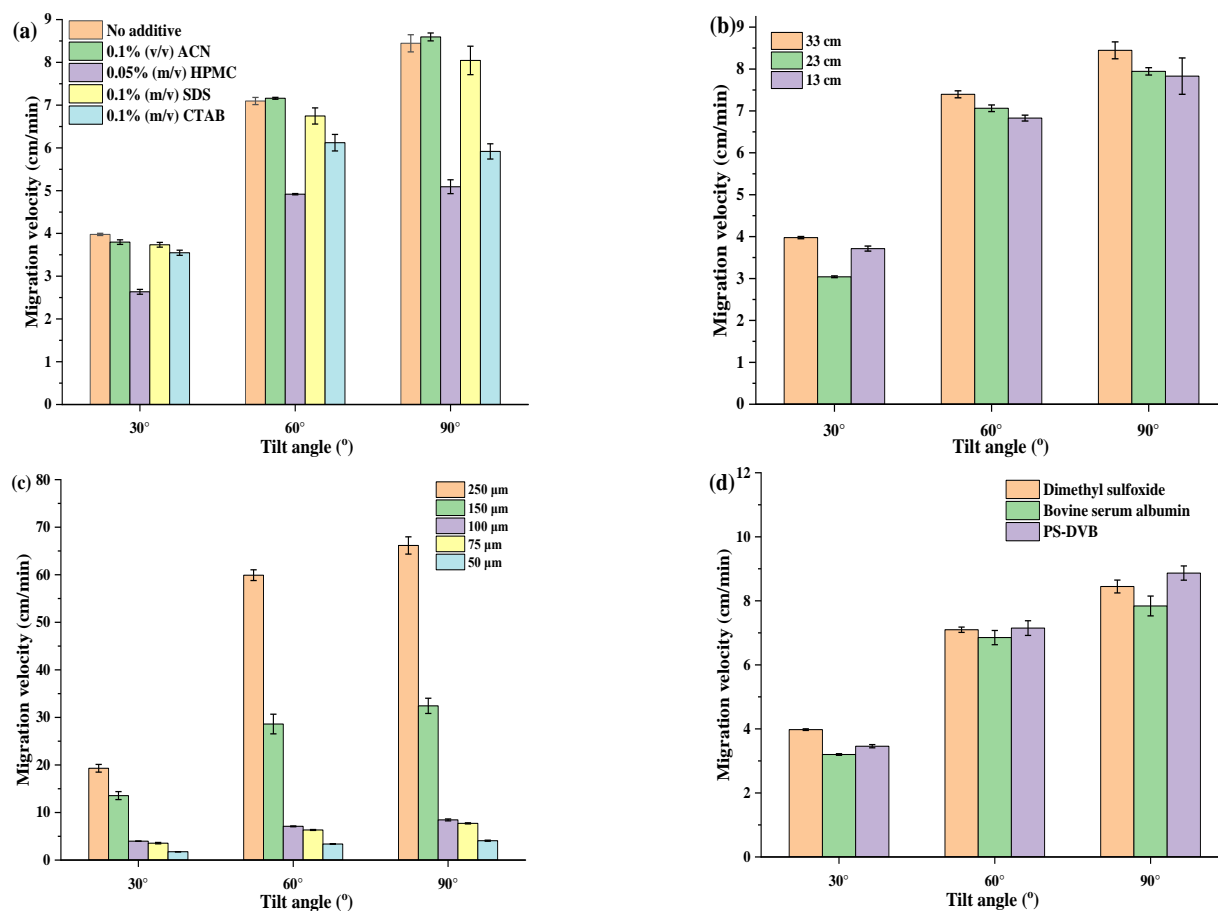


Figure 3. (a) Effect of additives on gravity effect. (b) Effect of capillary length on gravity effect. (c) Effect of capillary inner diameter on gravity effect. (d) Effect of sample size on gravity effect.

4.2. Validation of the Gravity-Mediated Capillary Electrophoresis

Under the fixed conditions excepting the capillary tilt angle, the apparent mobility in Equation (7), is simply written as the following formula:

$$y = a + b \sin \frac{\pi \theta}{180^\circ} \quad (8)$$

where y is μ_{ap-g} , a is the sum of μ_{EOF} and μ_{ep} , b is G' . The measured apparent mobility at different tilt angles could be processed using a simulation software (1stOpt15PRO).

After investigation of various parameters, the apparent mobilities of both aniline (positively charged) and p-toluene sulfonic acid (negatively charged) at different tilt angles were measured. Results were shown in Figure 4a. Data showed that when the B end of the capillary was upward, the fitting curves of apparent mobilities were $y = 4.725 + 7.116 \sin(\theta\pi/180^\circ)$ for aniline, and $y = 0.394 + 7.113 \sin(\theta\pi/180^\circ)$ for p-toluenesulfonic acid, corresponding to R^2 of 97.0% and 97.3%, respectively. When the B end of the capillary was downward, their fitting curves changed to $y = 4.063 - 8.068 \sin(\theta\pi/180^\circ)$ and $y = 0.260 - 8.969 \sin(\theta\pi/180^\circ)$. Their R^2 (98.4% and 98.7%) were always satisfactory. These results indicated the following information: First, when the direction of the gravity effect was the same as the migration direction, the apparent mobility increased gradually. Second, the curves for both compounds followed roughly the same trend with each of them having a mirror image relationship along a horizontal line passing the non-tilt position. Third, one zero mobility point for each compound was observed and the direction of the mobility reversed after passing the ZM point. Fourth, the mobilities between the two ZM points were in opposite directions. In addition, the outcome matched with the predictions of Equation (8) very well, which could obtain a fitting curve of mobility for each analyte.

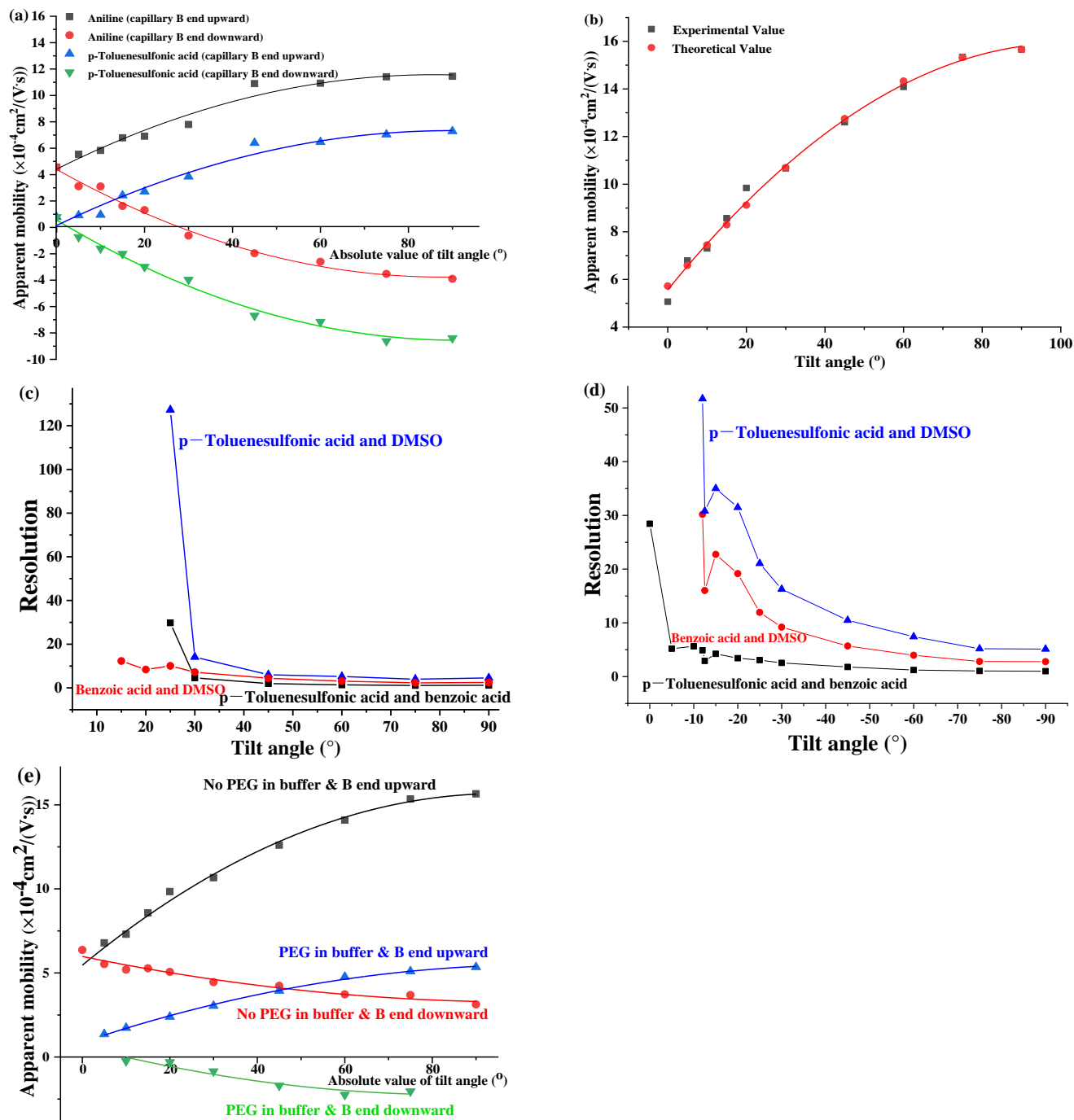


Figure 4. (a) Effect of tilt angle on mobility changes of aniline and p-toluenesulfonic acid ($n = 3$) and their formulas after fitting. (b) The fitting curve of the theoretical mobility value and the experimental mobility value of DMSO ($n = 3$). (c) Effect of capillary tilt angle (B end: upward) on the migration behavior of DMSO, benzoic acid and p-toluenesulfonic acid ($n = 3$). (d) Effect of tilt angle (B end: downward) on the migration behavior of DMSO, benzoic acid and p-toluenesulfonic acid ($n = 3$). (e) The comparison in apparent mobility of DMSO before and after adding PEG ($n = 3$).

Once the fitting curve of mobility was established on the limited measurements, in theory, it can be used to estimate the mobility at any angle. This is extremely useful for certain angles that may be difficult to measure experimentally. To verify this, DMSO was used as the model molecule and the results were summarized in Figure 4b. The experimental values and the theoretical prediction values were very close in its mobility curve ($y = 5.722 + 9.939\sin(\theta\pi/180^\circ)$). The fitting value was up to 99.1%, which further

validated the basic theory in Equation (8). Thus, it can be directly employed in CE. The mobility curve predicted the gravity effect from the following aspects: (1) an increase in velocity of migration when the gravity effect was in the same direction with EOF; (2) a decrease in velocity if the gravity effect was opposite; (3) holding a specific compound being static at a specific angle; or (4) two compounds migrating in opposite direction.

To validate these predictions experimentally, the mobilities between 0 to 90° and 0 to −90° for a mixture of three compounds, p-toluene sulfonic acid, benzoic acid and DMSO were measured. Figure S5 showed their typical electropherograms when the B end of the capillary was upward and the tilt angle gradually increased. When the tilt angle was zero, only DMSO, a neutral marker, was seen within 60 min. The other negatively charged compounds did not arrive at the detection window. When the angle reached from 10° to 25°, the benzoic acid and p-toluene sulfonic acid successively appeared at the detection window. This indicated that the compounds with reverse apparent mobilities in conventional CE migrated simultaneously toward the detection window when the gravity effect was used in CE. This saved sample, time and cost. At the same time, the effect of the gravity effect on resolution was also evaluated. Results (see Figure 4c) demonstrated that the most effective separation was between 0~30° for this specific separation. Angles bigger than 30° would totally overpower EOF, resulting in poor or no separation. A similar trend was observed when samples were injected with the downward B end of the capillary (Figure S6). A capillary tilt angle in the range of 0~−12° was useful for the separation (see Figure 4d). It was worth noting that the range of the useful tilt angle could be increased by coating the surface of the capillary or by adding polymers, such as polyethylene glycol (PEG) and hydroxyethyl cellulose (HEC), into the buffer solution. In this paper, we tried to add polymer into the buffer. As the viscosity increased, the apparent mobility was lowered by roughly 5 units by PEG (Figure 4e). The fitting curves of DMSO changed from $y = 5.722 + 9.939\sin(\theta\pi/180^\circ)$ for the upward B end of capillary, and $y = 5.934 - 2.588\sin(\theta\pi/180^\circ)$ for the downward B end of capillary to $y = 0.937 + 4.347\sin(\theta\pi/180^\circ)$ and $y = 0.415 - 2.777\sin(\theta\pi/180^\circ)$. Their R^2 were 99.07%, 94.78%, 99.86% and 93.89%, respectively. This provided an opportunity to use polymers to adjust the apparent mobility for a different separation purpose. Figure 4e also showed that the EOF was always substantial and did not reach 0 under normal conditions. With PEG, the overall EOF was lowered and reached 0 at −12.4°. When the tilt angle was lower than −12.4°, the sample migrated in the opposite direction. Further, even compounds that usually migrated to the A end of capillary migrated in the reverse direction after PEG addition.

4.3. Evaluation and Applications of the Gravity-Mediated Capillary Electrophoresis

4.3.1. Separation of Proteins

CE is especially suitable for the separation of proteins due to its high efficiency. To further evaluate the developed CE, ribonuclease A (RNase A, 1.0 mg/mL) and lysozyme (LZ, 1.0 mg/mL) were employed as model proteins. Since both of the proteins were positively charged and the injection end was B end of capillary (Figure 2), capillary tilt angles of 0~60° were tried first. The results were summarized in Figure S7. At 0°, lysozyme and ribonuclease A were observed in 8.298 min and 13.223 min, respectively. Their resolution was 3.691. With the increase of capillary tilt angles, the migration times were gradually shortened. At 60°, the migration times of the two proteins were 4.648 min and 5.540 min, and the resolution was reduced to 0.744. This indicated that the gravity effect broke the good separation which had established in non-capillary tilt mode. Then, capillary tilt angles of 0~−30° were investigated and data were listed in Figure 5a. The results showed the migration times of the two proteins were prolonged and resolutions (R_s) were significantly improved from 3.691 to 5.108 at −20°. At −30°, the peak of ribonuclease A was not observed during 50 min. To analyze the reason of change in migration and resolution, more detailed apparent mobilities of proteins at different capillary tilt angles of 0~+75° and 0~−70° were investigated. The data were summarized in Figure 5b, which were fitted to Equation (8). The fitting curves of lysozyme were $y = 3.139 + 2.806\sin(\theta\pi/180^\circ)$ for the

upward B end of capillary and $y = 3.414 - 4.850\sin(\theta\pi/180^\circ)$ for the downward B end of capillary, corresponding to R^2 of 96.8% and 97.1%, respectively. Similarly, the fitting curve of ribonuclease A was $y = 2.040 + 2.988\sin(\theta\pi/180^\circ)$ or $y = 2.171 - 3.986\sin(\theta\pi/180^\circ)$ under the upward or downward B end of capillary, corresponding to R^2 of 98.5% and 96.1%, respectively. All the R^2 values of fitting curves were more than 96%. This proved the developed CE theory helpfully reflected the migration behavior, and even proteins of the analytes. It further verified the blind use of gravity or pressure may produce an opposing effect. Phase 2 in Figure 1 was a useful range of capillary tilt angle. Thus, the proposed theory of new CE technology was very instructive.

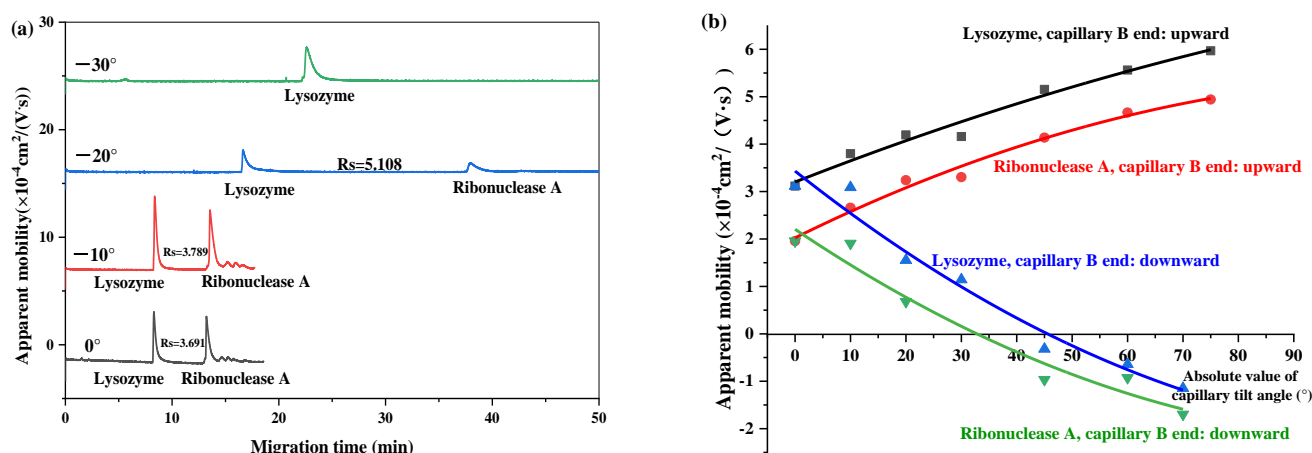


Figure 5. (a) Typical electropherograms of lysozyme and ribonuclease A at $0\sim 40^\circ$ of capillary tilt angles. (b) Apparent mobilities of lysozyme and ribonuclease A at different angles ($n = 3$) and their fitting formulas.

4.3.2. Separation of Chiral Compounds

CE is often used in chiral separation. To evaluate the effectiveness of the novel CE technology, we attempted to separate terbutaline and lactic acid enantiomers. The results were shown in Figure 6a–d. As the positive tilt angle increased, the migration velocities of terbutaline enantiomers slowed down from 7.80 min and 8.82 min to 16.940 min and 21.015 min (see Figure 6a). It was speculated that the gravity portion slowed down the migration velocity of SPE- β -CDP and prolonged the interaction time between SPE- β -CDP and terbutaline enantiomers. As the tilt angle increased from 0° to 20° , their resolution significantly increased from baseline separation (1.303) to complete separation (2.151). The results indicated that the introduced gravity was useful. However, when the capillary tilt angle was too large, it made the peak deformation wider. Thus, it was necessary to study a suitable range of tilt angle according to the specific target. Terbutaline data were further used to validate the Equation (8), whose apparent mobilities at different capillary tilt angles were shown in Figure 6b. Their fitting curves were $y_1 = 2.486 - 4.119 \sin(\pi\theta/180^\circ)$ and $y_2 = 2.135 - 3.749 \sin(\pi\theta/180^\circ)$. The R^2 values of curves were 98.7% and 97.3%, respectively, indicating the Equation (8) was suitable for describing the variation of the apparent mobility of the enantiomers as the capillary tilt angle.

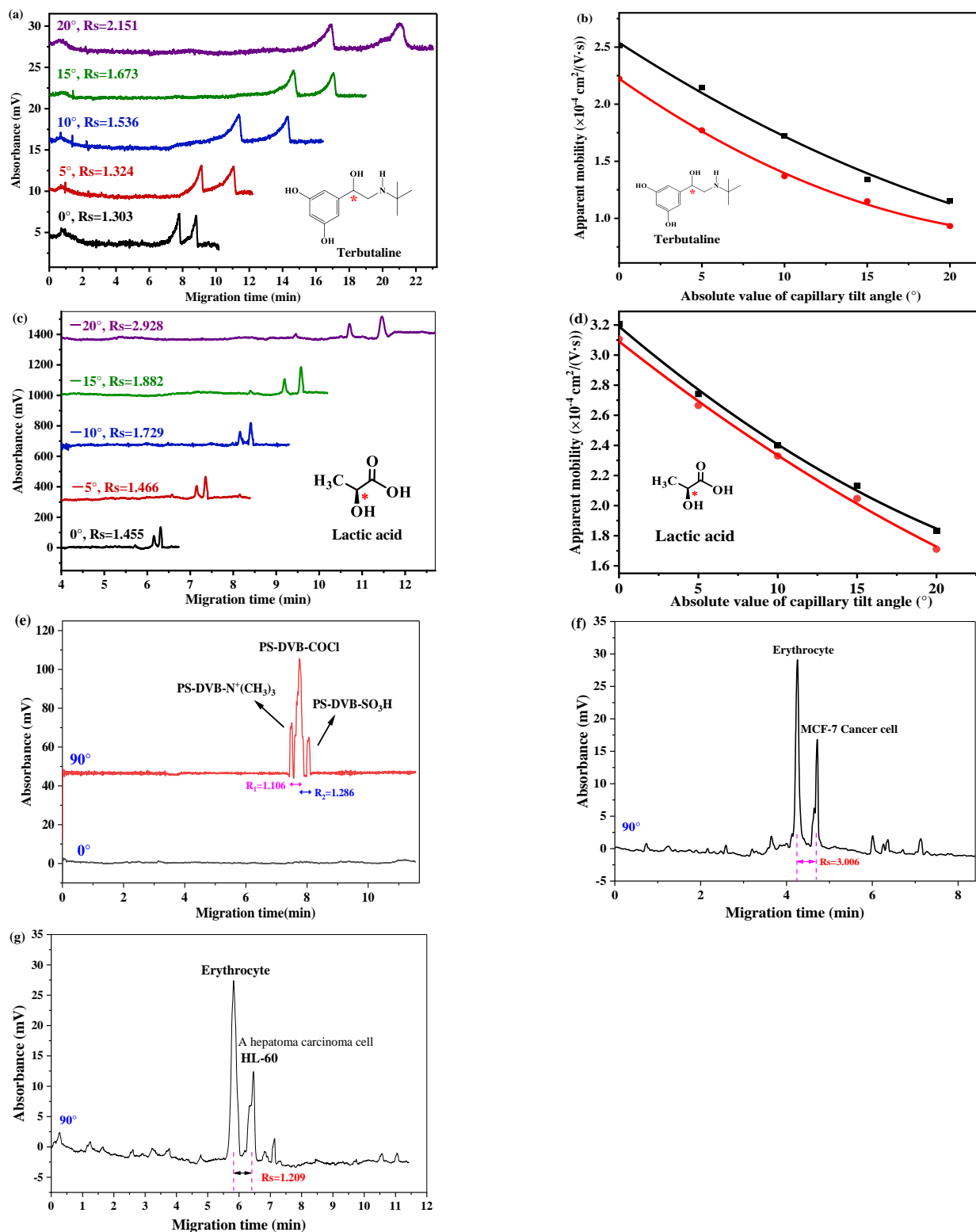


Figure 6. (a) Typical electropherograms of terbutaline at different tilting angles of capillary. (b) Apparent mobilities of terbutaline enantiomers at different capillary tilting angles ($n = 3$) and their fitting formulas. (c) Typical electropherograms of lactic acid at different tilting angles of capillary. (d) Apparent mobilities of lactic acid enantiomers at different capillary tilting angles ($n = 3$) and their fitting formulas. (e) Typical electropherograms of 5 μm microspheres at horizontal angle and vertical angle. (f) Typical electropherograms of MCF-7 breast cancer cell and (g) HL-60 hepatoma carcinoma cell from erythrocyte under 90°. “*” means that is a chiral carbon.

From the lactic acid data shown in Figure 6c, the resolutions of the enantiomers were apparently affected by capillary tilt angles. When they changed from 0° to -20° , the resolutions significantly improved from 1.455 to 2.928. This was because the effective electrophoretic mobility of SPE- β -CDP was reduced, and the interaction time with SPE- β -CDP was extended, thus resulting in the improved separation. After calculating their apparent mobilities at different capillary tilt angles and fitting curves to Equation (8), it was obvious that they had very satisfactory results (see Figure 6d). Their fitting curves were $y_1 = 3.139 - 3.928\sin(\pi\theta/180^\circ)$ and $y_2 = 3.059 - 3.987\sin(\pi\theta/180^\circ)$. The R^2 values of curves were up to 99.7% and 99.4%, respectively. They again verified the theory of novel CE technology.

4.3.3. Separation of Microspheres and Cells by Gravity Effect

In the field of life sciences, there are many big analytes, such as micron-sized cells. They were never analyzed by traditional CE. This became possible by utilizing gravity in CE, and was investigated through employing PS-DVB-COCl, PS-DVB-SO₃H, and PS-DVB-N⁺(CH₃)₃ microspheres of 5 μ m as model samples. The results were shown in Figure 6e. When the capillary was at the horizontal, the microspheres were difficult to move in the capillary under the electric drive because of their large size and relatively low charge. The precipitation issue further hindered their migration toward the detection window. When the capillary was changed to a vertical angle and gravity effect was utilized as the third force, three kinds of microspheres with different charged properties migrated to the detection window under gravity effect. Due to the obvious gravity effect at 90° , their column efficiencies were very high, corresponding to 175,100/m, 41,872/m, and 156,672/m for PS-DVB-N⁺(CH₃)₃, PS-DVB-COCl and PS-DVB-SO₃H microspheres, respectively. Their resolutions were 1.106 and 1.286, respectively. Similarly, gravity-mediated CE technology was also used to preliminary separate cancer cells (MCF-7 and HL-60) from erythrocyte which was given by Professor Zichuan Liu. The results were shown in Figure 6f,g. Their resolutions could be up to 3.006 and 1.209, which was the first successful separation of cells. The successful application in microspheres and cells showed that this method was also effective for the separation of micrometer level analytes.

4.4. Gradient Capillary Electrophoresis and Its Application Strategy

4.4.1. The Design Mentality for Gradient Capillary Electrophoresis

In theory, it is possible to change the capillary tilt angle over time to adjust the apparent mobility of the analyst. Although this method may improve separation, especially for separating two otherwise difficult-to-separate compounds, the migration would be relatively slow when parts of mobility were offset by the gravity effect. Thus, a short separation path would be needed. This may be advantageous in some situations, such as microchips, but may also be difficult in regular CE, where it would take long time and result in broad peaks of compounds. To overcome this problem, a novel gradient electrophoresis process by dynamically changing the gravity effect was proposed and evaluated.

A three-stage gradient capillary electrophoresis (GCE) process was shown in Figure 7a. In the first stage (blue area) of GCE, the capillary was tilted at angle (1), and compound A and compound B migrated toward the detection window at different velocities. The cut-off time (t_1) of the first stage should be dictated by neither compound having arrived at the detection window. Then, another tilt angle (2) (yellow area) was adopted for the second stage. Angle (2) was within phase 2 (Figure 1), where the velocities of at least one of the compounds reached the net zero mobility point or they had an opposite migration direction. Then, one compound migrated while the other stopped or they migrated in opposite directions. This process stopped at time t_2 or when the compound in front arrived at, or passed, the detection window (t_3 or t_4). This stage was the separation enhancement stage where the longer the time, the greater the separation efficiency. However, this process had to be limited to a certain time to make sure that the compound going in the opposite direction did not come out from the injection end or to avoid the band of the stopped

compound broadening. To ensure all of the compounds migrated toward the detection window, the capillary tilt angle needed to be adjusted again so that it would start the third stage (green area) with angle (3), where elevating the angle would allow the compounds to migrate rapidly across the detection window.

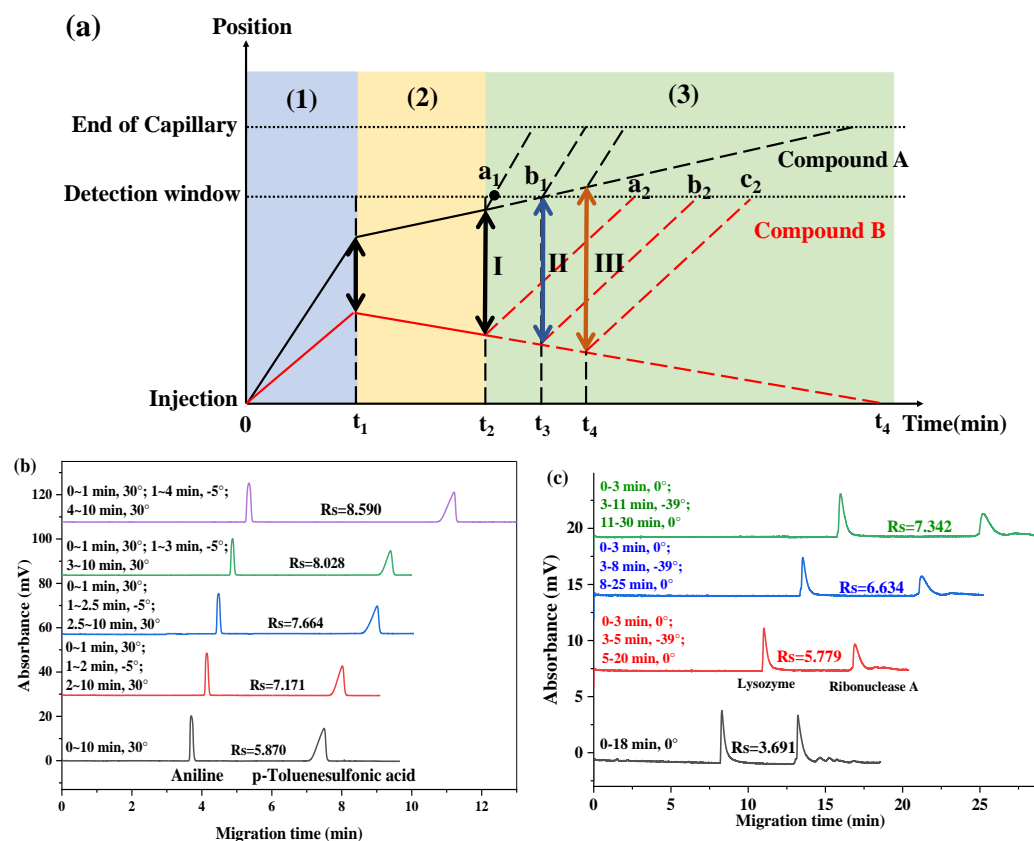


Figure 7. (a) Schematic diagram of the three stages of gradient CE mode. (b) Effect of the duration time at Phase 2 on separation of aniline and p-toluenesulfonic acid. (c) Separation efficiencies of lysozyme and ribonuclease A under gradient CE mode.

In GCE, the efficiency of separation was controlled by the second stage. There are three situations: (1) neither compound arrived at the detection window, time t_2 was cut-off and the migration time of the two compounds corresponds to a_1 and a_2 , respectively; (2) the capillary tilt angle was switched into the third stage when the first compound arrived at the detection window, and the migration time of the two compounds was the time corresponding to b_1 and b_2 , respectively; (3) the third stage started when the first compound had passed through the detection window. Their migration times corresponded to b_1 and c_2 , respectively. By comparing the distance between a_2 and a_1 , b_2 and b_1 , c_2 and b_1 , the change in the resolution of the compounds could be observed.

In GCE, three factors have to be considered: (1) the specific tilt angles, (2) the time point to change the capillary tilt angle, and (3) the duration of each stage. The angles of stage 1 and stage 3 were easy to determine, as all of the angles where the two compounds migrated to the detection window with a fast speed were available. The specific angle of stage 2 was chosen for the two compounds migrating in opposite directions. The duration of the second stage needed to be pre-determined.

4.4.2. The Validation of Gradient Capillary Electrophoresis

To validate this gradient mentality, a series of experiments were designed. The sample was a mixture of p-toluenesulfonic acid and aniline. It was proved that under these conditions (see Figure 4a), and with an upward capillary tilt angle, such as 30° , both aniline and p-toluenesulfonic acid would migrate from the B end to A end of the capillary

with $\mu_{\text{aniline}} > \mu_{\text{p-toluenesulfonic acid}}$ (see Figure 2). When angled at -5° – -25° , aniline would also migrate from the B end to A end of the capillary but at a slower speed, while p-toluenesulfonic acid began to migrate in the opposite direction under the synergistic effect of the gravity effect and the electric force. Thus, at -30° , the two compounds migrated to the A end of the capillary, and the distance between aniline and p-toluenesulfonic acid steadily increased. In the second stage when the angle was lowered to -5° , the two compounds migrated to the opposite direction, which was equivalent to dynamically extending the distance between them. If the time of the second stage continued to extend, the resolution could be further extended. Thus, a strategy for designing a GCE experiment was illustrated in Figure 7b. It showed the effect of the opposite migration time on their separations. If the duration time in stage 2 changed, it was significant to increase the length of the opposite migration and the separation efficiency. With the prolonging of the duration time, the distance between aniline and p-toluenesulfonic acid increased, and their migration times also increased. Their resolutions also increased from 5.870 to 8.590. The experimental results were consistent with the expectations.

4.4.3. Separation of Proteins by the Gradient Capillary Electrophoresis

Both lysozyme and ribonuclease A were employed as model samples. From their fitting curves in Figure 5b, the apparent mobilities of lysozyme and ribonuclease A at 0° and 30° could be calculated. When the angle of the capillary was 0° , the migration velocity of lysozyme was 4.399 cm/min, and ribonuclease A was 3.502 cm/min. When the angle was 30° , the two were 6.710 cm/min and 5.869 cm/min, respectively. The direct comparison between theoretical and experimental migration times (Figure S8) revealed that they were consistent, and the new theory could predict the migration of the targets.

To further utilize special angles to improve resolution, GCE was employed to improve the separation of the two proteins. Substituting the mobility 0 into the derived fitting curves in Figure 5b, it was known that the angle of lysozyme was -44.742° , and lysozyme A was -33.001° . The middle angle between the two was -38.871° , where the two proteins moved in opposite directions. After a series of gradient capillary electrophoresis, results were summarized in Figure 7c. It showed that resolutions of lysozyme and ribonuclease A were greatly improved from 3.691 to 7.342, which showed good potential in separating macromolecules.

4.4.4. Separation of Chiral Compounds by Gradient Capillary Electrophoresis

The further separation of lactic acid and terbutaline enantiomers were also tried using the novel GCE. The results were shown in Figure 8.

For lactic acid enantiomers, if the fitting curves are ignored during the design of the gradient program, an improvement in separation efficiency may be obtained through the investigation of capillary tilt angle data. For example, the migration time of the first stage was 0–3 min at 0° . The duration time of the second stage was 3–11 min at -30° , -40° , or -50° , respectively. The capillary tilt angle in the third stage was back to 0° until the end of process. The results were shown in Figure 8a. It could be seen that as the angle of the second stage decreased, the resolutions of the two lactic acid enantiomers gradually increased from 1.455 to 3.946. It showed that gradient capillary electrophoresis technology could effectively improve the separation of lactic acid enantiomers. If the fitting curves shown in Figure 6d were used in gradient design, it could be observed there were two zero mobilities, at -50° and -53° , respectively. The best result in Figure 8a was from the zero mobility of one enantiomer, which was fortunately designed in the second stage of the gradient capillary electrophoresis. If it was only set up at -40° , the maximum resolution was only 3.028, which was similar to the 2.928 shown in Figure 6c. This could easily lead to a misinterpretation of the separation ability of gradient capillary electrophoresis. This reminded us that the closer to the zero point, the higher the resolutions of lactic acid enantiomers. Thus, it was necessary to redesign the gradient program according to the two zero mobilities at -50° and -53° . At the middle value of -51.5° , they could migrate

in opposite directions. The detailed gradient programs and results were summarized in Figure 8b. It was obvious that the resolutions were greatly increased to 5.180 and 5.920 when the duration times in the second stage were 12 min and 13 min, respectively. This led us to conclude that both time-gradient and angular gradient capillary electrophoresis had good adjustability and simple operation.

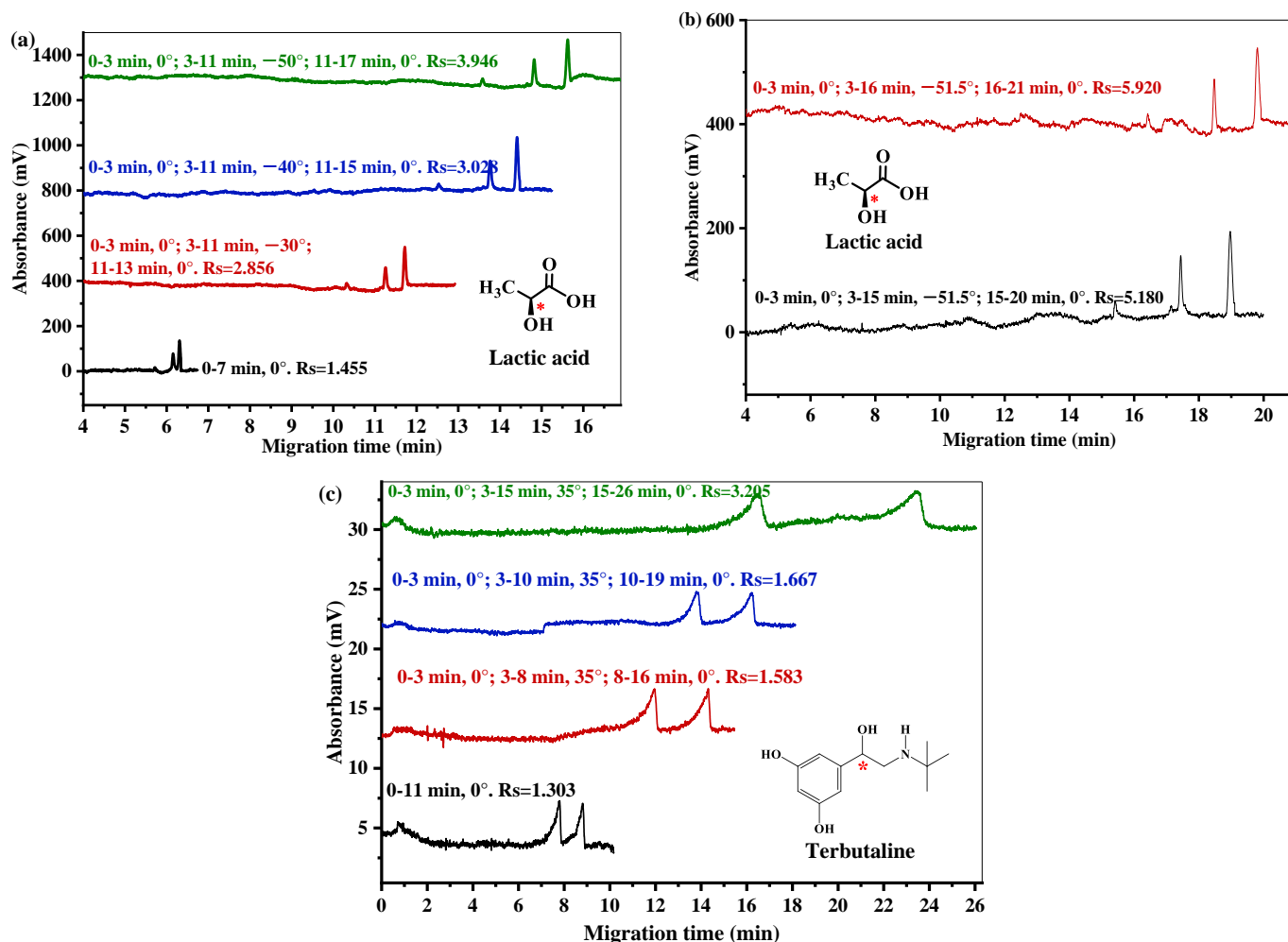


Figure 8. (a) Typical electropherograms of lactic acid enantiomers under different capillary tilt angles at different duration times. (b) Typical electropherograms of lactic acid enantiomers under different duration times of capillary tilt angles. (c) Typical electropherograms of terbutaline enantiomers under gradient CE mode. “*” means that is a chiral carbon.

Similarly, through extending the fitting curves in Figure 6b, it turned out that one of the terbutaline enantiomers had a zero mobility at 34°, and the other had a zero mobility at 37°. At the middle value of 34–37°, they could migrate in opposite directions. After designing and executing gradient electrophoresis at 35° as the gradient point, the results were shown in Figure 8c. The data also showed that the longer the duration time at zero mobility, the higher the resolution of the terbutaline two enantiomers. Their resolution was improved from 1.303 to 3.205, which was higher than the simple change in capillary tilt angle ($R_s = 2.151$). It indicated that the gradient capillary electrophoresis could be more effective. The new gradient CE mode provided a new strategy for the separation of compounds.

5. Conclusions

A gravity effect basing the vector sum of gravity and buoyancy force, or their portion as another force, was introduced into CE. The related formula was proposed and validated

through experiments, which improved separation when the tilt angle fell in the suitable range (Phase 2 in Figure 1). It also could make different ions with greatly different mobilities be observed at a CE run. A gradient CE mode was also proposed and verified. Experiment results showed the gravity effect mediated CE, and its gradient mode could improve the separation effect of small molecules, proteins, chiral enantiomer, and even particles and cells. These results indicate that this technology has huge application potential.

Supplementary Materials: The following supporting information can be downloaded at: <https://www.mdpi.com/article/10.3390/separations11120340/s1>.

Author Contributions: W.J.: Formal analysis, Investigation, Validation, Writing—original draft. P.Z.: Investigation, Validation. Y.C.: Validation. J.J.B.: Supervision, Writing—review and editing. Y.X.: Validation, Writing—review and editing. Y.L.: Conceptualization, Funding acquisition, Project administration, Supervision, Writing—review and editing. All authors have read and agreed to the published version of the manuscript.

Funding: National Natural Science Foundation of China under grant (No. 21605112).

Data Availability Statement: The data that support the findings of this paper are available from the corresponding author upon reasonable request.

Conflicts of Interest: The authors declare no conflicts of interest.

References

- Jorgenson, J.W.; Lukacs, K.D. High-resolution separations based on electrophoresis and electroosmosis. *J. Chromatogr. A* **1981**, *218*, 209–216. [\[CrossRef\]](#)
- Jorgenson, J.W.; Lukacs, K.D. Zone electrophoresis in open-tubular glass capillaries: Preliminary data on performance. *J. High Resolut. Chromatogr.* **1981**, *4*, 230–231. [\[CrossRef\]](#)
- Hayes, M.A.; Kheterpal, I.; Ewing, A.G. Electroosmotic flow control and surface conductance in capillary zone electrophoresis. *Anal. Chem.* **1993**, *65*, 2010–2013. [\[CrossRef\]](#) [\[PubMed\]](#)
- Yao, X.W.; Wu, D.; Regnier, F.E. Manipulation of electroosmotic flow in capillary electrophoresis. *J. Chromatogr.* **1993**, *636*, 21–29. [\[CrossRef\]](#)
- Kasicka, V.; Prusik, Z.; Sazelova Brynda, E.; Stejskal, J. Capillary zone electrophoresis with electroosmotic flow controlled by external radial electric field. *Electrophoresis* **1999**, *20*, 2484–2492. [\[CrossRef\]](#)
- Lee, C.S.; McManigill, D.; Wu, C.T.; Patel, B. Factors affecting direct control of electroosmosis using an external electric field in capillary electrophoresis. *Anal. Chem.* **1991**, *63*, 1519–1523. [\[CrossRef\]](#)
- Lee, C.S.; Blanchard, W.C.; Wu, C.T. Direct control of the electroosmosis in capillary zone electrophoresis by using an external electric field. *Anal. Chem.* **1990**, *62*, 1550–1552. [\[CrossRef\]](#)
- Hong, S.; Lee, C.S. Electroosmotic control of chiral separation in capillary zone electrophoresis. *Electrophoresis* **1995**, *16*, 2132–2136. [\[CrossRef\]](#)
- Williams, B.A.; Vigh, G. Fast, accurate mobility determination method for capillary electrophoresis. *Anal. Chem.* **1996**, *68*, 1174–1180. [\[CrossRef\]](#)
- Wu, C.T.; Lopes, T.; Patel, B.; Lee, C.S. Effect of direct control of electroosmosis on peptide and protein separations in capillary electrophoresis. *Anal. Chem.* **1992**, *64*, 886–891. [\[CrossRef\]](#)
- Tsai, P.; Patel, B.; Lee, C.S. Direct control of electroosmosis and retention window in micellar electrokinetic capillary chromatography. *Anal. Chem.* **1993**, *65*, 1439–1442. [\[CrossRef\]](#)
- Karni, Z.; Kopito, L.E. Magneto-electrophoresis. *Med. Biol. Eng. Comput.* **1975**, *13*, 457–462. [\[CrossRef\]](#) [\[PubMed\]](#)
- Razee, S.; Tamura, A.; Masujima, T. The effect of a crossed magnetic field on capillary electrophoresis. *Chem. Pharm. Bull.* **1994**, *42*, 2376–2378. [\[CrossRef\]](#)
- Beckers, J.L.; Bocek, P. Multiple effect of surfactants used as additives in background electrolytes in capillary zone electrophoresis: Cetyltrimethylammonium bromide as example of model surfactant. *Electrophoresis* **2002**, *23*, 1947–1952. [\[CrossRef\]](#) [\[PubMed\]](#)
- Doherty, E.A.S.; Meagher, R.J.; Albarghouthi, M.N.; Barron, A.E. Microchannel wall coatings for protein separations by capillary and chip electrophoresis. *Electrophoresis* **2003**, *24*, 34–54. [\[CrossRef\]](#)
- de Bellaistre, M.C.; Randon, J.; Rocca, J.L. Hydrodynamic flow and electroosmotic flow in zirconia-packed capillaries. *Electrophoresis* **2006**, *27*, 736–741. [\[CrossRef\]](#)
- Tian, M.; Wang, Y.; Mohamed, A.C.; Guo, L.; Yang, L. Enhancing separation in short-capillary electrophoresis via pressure-driven backflow. *Electrophoresis* **2015**, *36*, 1549–1554. [\[CrossRef\]](#)
- Xia, L.; Dutta, D. Microchip-based electrophoretic separations with a pressure-driven backflow. *Methods Mol. Biol.* **2019**, *1906*, 239–249.
- Xia, L.; Dutta, D. Microfluidic flow counterbalanced capillary electrophoresis. *Analyst* **2013**, *138*, 2126–2133. [\[CrossRef\]](#)

20. Han, C.; Sun, J.; Liu, J.; Cheng, H.; Wang, Y. A pressure-driven capillary electrophoretic system with injection valve sampling. *Analyst* **2015**, *140*, 162–173. [[CrossRef](#)]
21. Gordon, G.B. Electroosmotic Flow Control Using Back Pressure in Capillary Electrophoresis. U.S. Patent No. US-5429728-A, 23 September 1995.
22. Muzikar, J.; van de Goor, T.; Gas, B.; Kenndler, E. Determination of electroosmotic flow mobility with a pressure-mediated dual-ion technique for capillary electrophoresis with conductivity detection using organic solvents. *J. Chromatogr. A* **2002**, *960*, 199–208. [[CrossRef](#)] [[PubMed](#)]
23. Masar, M.; Hradski, J.; Schmid, M.G.; Szucs, R. Advantages and pitfalls of capillary electrophoresis of pharmaceutical compounds and their enantiomers in complex samples: Comparison of hydrodynamically opened and closed systems. *Int. J. Mol. Sci.* **2020**, *21*, 6852. [[CrossRef](#)] [[PubMed](#)]
24. Williams, B.A.; Vigh, G. Determination of effective mobilities and chiral separation selectivities from partially separated enantiomer peaks in a racemic mixture using pressure-mediated capillary electrophoresis. *Anal. Chem.* **1997**, *69*, 4410–4418. [[CrossRef](#)] [[PubMed](#)]
25. Cai, H.; Vigh, G. Method for the elimination of chromatographic bias from measured capillary electrophoretic effective mobility values. *Anal. Chem.* **1998**, *70*, 4640–4643. [[CrossRef](#)] [[PubMed](#)]
26. Glukhovskiy, P.V.; Vigh, G. A simple method for the determination of isoelectric points of ampholytes with closely spaced pKa values using pressure-mediated capillary electrophoresis. *Electrophoresis* **1998**, *19*, 3166–3170. [[CrossRef](#)]
27. Soga, T.; Ueno, Y.; Naraoka, H.; Matsuda, K.; Tomita, M.; Nishioka, T. Pressure-assisted capillary electrophoresis electrospray ionization mass spectrometry for analysis of multivalent anions. *Anal. Chem.* **2002**, *74*, 6224–6229. [[CrossRef](#)]
28. Mai, T.D.; Hauser, P.C. Pressure-assisted capillary electrophoresis for cation separations using a sequential injection analysis manifold and contactless conductivity detection. *Talanta* **2011**, *84*, 1228–1233. [[CrossRef](#)]
29. Soga, T.; Ishikawa, T.; Igarashi, S.; Sugawara, K.; Kakazu, Y.; Tomita, M. Analysis of nucleotides by pressure-assisted capillary electrophoresis-mass spectrometry using silanol mask technique. *J. Chromatogr. A* **2007**, *1159*, 125–133. [[CrossRef](#)]
30. Vanifatova, N.G.; Rudnev, A.V.; Gabrielyan, G.A.; Dzhenloda, R.K.; Burmistrov, A.A.; Lazareva, E.V.; Dzherayan, T.G. Application of pressure in capillary zone electrophoresis to study the aggregation of chitosan 2-hydroxybutoxypropylcarbamate. *J. Anal. Chem.* **2017**, *72*, 803–809. [[CrossRef](#)]
31. Zhang, B.; Li, Y.X.; Gao, H.N.; Bian, J.; Bao, J. Rapid determination of protein binding constant by a pressure-mediated affinity capillary electrophoresis method. *Electrophoresis* **2011**, *32*, 3589–3596. [[CrossRef](#)]
32. Qian, C.; Wang, S.; Fu, H.; Turner, R.F.B.; Li, H.; Chen, D.D.Y. Pressure-assisted capillary electrophoresis frontal analysis for faster binding constant determination. *Electrophoresis* **2018**, *39*, 1786–1793. [[CrossRef](#)] [[PubMed](#)]
33. Golab, M.; Wozniakiewicz, M.; Nowak, P.M.; Koscielniak, P. An automated hydrodynamically mediated technique for preparation of calibration solutions via capillary electrophoresis system as a promising alternative to manual pipetting. *Molecules* **2021**, *26*, 6268. [[CrossRef](#)] [[PubMed](#)]
34. Kanoatov, M.; Retif, C.; Cherney, L.T.; Krylov, S.N. Peak-shape correction to symmetry for pressure-driven sample injection in capillary electrophoresis. *Anal. Chem.* **2012**, *84*, 149–154. [[CrossRef](#)] [[PubMed](#)]
35. Williams, B.A. Terra Incognita: Pressure-Mediated Capillary Electrophoresis with Strategic Band Transfer. Ph.D. Thesis, A&M University, College Station, TX, USA, 2017; pp. 97–100.
36. Culbertson, C.T.; Jorgenson, J.W. Flow counterbalanced capillary electrophoresis. *Anal. Chem.* **1994**, *66*, 955–962. [[CrossRef](#)]
37. Wang, W.; Zhou, F.; Wu, W. A micro-electrophoresis system based on a short capillary with hydrostatic pressure assisted separation and injection. *Microchim. Acta* **2009**, *166*, 35–39. [[CrossRef](#)]
38. Kar, S.; Dasgupta, P.K. Improving resolution in capillary zone electrophoresis through bulk flow control. *Microchem. J.* **1999**, *62*, 128–137. [[CrossRef](#)]
39. Nan, Y.Q.; Zheng, P.Y.; Cheng, M.Q.; Zhao, R.; Jia, H.J.; Liang, Q.G.; Li, Y.X. Enhancement of chiral drugs separation by a novel adjustable gravity mediated capillary electrophoresis combined with sulfonic propyl ether β -CD polymer. *Anal. Chim. Acta* **2023**, *1279*, 341781. [[CrossRef](#)]

Disclaimer/Publisher’s Note: The statements, opinions and data contained in all publications are solely those of the individual author(s) and contributor(s) and not of MDPI and/or the editor(s). MDPI and/or the editor(s) disclaim responsibility for any injury to people or property resulting from any ideas, methods, instructions or products referred to in the content.